

78
9-4-79

10.3085
AUGUST 1979
PPPL-1579
UC-208

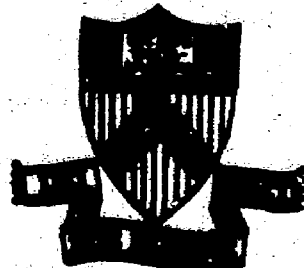
UNSTABLE UNIVERSAL DRIFT EIGENMODES
IN TOROIDAL PLASMAS

BY

C. Z. CHENG AND L. CHEN

MASTER

PLASMA PHYSICS
LABORATORY



DISTRIBUTION OF THIS DOCUMENT IS UNLIMITED

Unstable Universal Drift Eigenmodes in Toroidal Plasmas*

C. Z. Cheng and Liu Chen

Plasma Physics Laboratory, Princeton University
Princeton, New Jersey 08544

ABSTRACT

The eigenmode equation describing ballooning collisionless drift instabilities is analyzed both analytically and numerically. A new branch of eigenmodes, which corresponds to quasi-bound states due to the finite toroidicity, is shown to be destabilized by electron Landau damping for typical Tokamak parameters. This branch cannot be understood by the strong coupling approximation. However, the slab-like (Pearlstein-Berk type) branch is found to remain stable and experience enhanced shear damping due to finite toroidicity.

NOTICE

This report was prepared as an account of work sponsored by the United States Government. Neither the United States nor the United States Department of Energy, nor any of their employees, or any of their contractors, subcontractors, or their employees, makes any warranty, express or implied, or assumes any legal liability or responsibility for the accuracy, completeness or usefulness of any information, apparatus, product or process disclosed, or represents that its use would not infringe privately owned rights.

Rey

In slab geometry, both the collisionless and collisional electrostatic drift eigenmodes are found to be shear stabilized.¹ The shear damping of drift waves is associated with the anti-well structure in which energy convects away from the mode rational surface.² However, in a toroidal plasma the mode rational surfaces are closely packed. Due to toroidal coupling effects, such as magnetic curvature drifts, the eigenmodes of each poloidal harmonic are affected by the wave energy which is convected away from the neighboring mode rational surfaces. With finite toroidicity, the toroidal coupling effects can form local potential wells, which inhibit convection of wave energy, and hence significantly reduce the shear damping. The stability studies of drift waves in toroidal systems using Taylor's strong-coupling approximation³ have been carried out.⁴ It was found that drift wave eigenmodes are stable for typical shear values in tokomaks, $\hat{s} = rq'/q > 1/2$, where $q = rB_\phi/RB_\theta$ is the safety factor. However, the strong-coupling approximation, which requires large \hat{s} ($\hat{s} > 1/2$), does not correctly describe the formation of local potential wells. Recent studies of shear damping effects for two-dimensional drift wave eigenmodes⁵ in toroidal plasma using the ballooning mode formalism⁶ indicated that two branches of eigenmodes exist. One is slab-like and the other is a new branch induced by finite toroidicity. The slab-like branch, which represents the extension of Pearlstein-Berk slab eigenmodes², has anti-well potential structures. It corresponds to an unbounded state experiencing finite shear damping and exists for small toroidicity. On the other hand, the toroidicity induced eigenmode branch, which has no counterpart in slab geometry, is

characterized by potential structures with local potential wells. It corresponds to a marginally stable, quasi-bound state and experiences negligible shear damping through tunneling leakages. However, in reference 5, adiabatic electrons and cold fluid ions were employed. The crucial question on stability of the collisionless drift waves in toroidal plasmas is yet to be answered.

In the present work we keep dissipative effects such as electron and ion Landau damping by retaining the full electron and ion Z functions and adopt the ballooning mode formalism⁶ to investigate the stability properties of collisionless drift wave eigenmodes in toroidal plasmas. The toroidal coupling effects considered here are due to ion VB and curvature drifts.⁷ We find both analytically and numerically that the toroidicity-induced branch becomes absolutely unstable in the presence of electron Landau damping, while the slab-like branch experiences enhanced shear damping.

In the following we consider long wave length ($k_{\perp}r_i \ll 1$) electrostatic drift waves in a large aspect ratio ($\epsilon = a/R \ll 1$), axisymmetric tokamak with concentric, circular magnetic surfaces. The perturbation, Ψ , can be written in the form

$$\Psi(r, \theta, \xi, t) = \sum_j \hat{\phi}_j(s) \exp [i(m_o \theta + j\theta - n\xi - \omega t)] \quad (1)$$

where (r, θ, ξ) correspond to the minor radial, poloidal and toroidal directions respectively, $s = (r - r_o)/\Delta r_s$, r_o is the minor radius of the reference mode rational surface with $m_o = nq(r_o)$, $\Delta r_s = 1/k_\theta \hat{s}$, $k_\theta = m_o/r_o$, $\hat{s} = (rq'/q)_r = r_o$ and $|j| \ll |m_o|$. For simplicity, we ignore temperature gradients,

collisional and trapped particle effects. The two-dimensional eigenmode equation can be derived straightforwardly⁷ and is given by

$$[L(s, j) + \bar{Q}(s, j) - \epsilon_n T/\Omega] \hat{\phi}_j(s) = 0 \quad (2)$$

where

$$L = b_\theta (\hat{s}^2 d^2 / ds^2 - 1),$$

$$\bar{Q} = (1-\Omega) / (\Omega + 1/\tau) [1 + \xi_e z(\xi_e)] - \tau [1 + \xi_i z(\xi_i)],$$

$$T \hat{\phi}_j(s) = \hat{\phi}_{j+1}(s) + \hat{\phi}_{j-1}(s) + \hat{s} \frac{\partial}{\partial s} [\hat{\phi}_{j+1}(s) - \hat{\phi}_{j-1}(s)],$$

$$b_\theta = k_\theta^2 \rho_s^2, \tau = T_e / T_i, \rho_s = C_s / \omega_{ci}, C_s^2 = T_e / M_i,$$

$$\epsilon_n = r_n / R, r_n^{-1} = |d \ln N(r) / dr|, \xi_i = \sqrt{\tau/2} \Omega n_s / |s-j|,$$

$$\xi_e = \xi_i / d, d = \sqrt{M_e / M_i} \tau, n_s = q b_\theta^2 / \epsilon_n, z \text{ is the plasma}$$

dispersion function, and $\Omega = \omega / \omega_{*e}$. The operator T is due to the ion magnetic drifts.

Since, typically, $|m_0| \sim |n| \sim r_n / \rho_s \sim 0 (10^2)$, we may employ the large n ordering which leads to the ballooning mode formalism. In zeroth order, we have, with $z = s-j$, $\hat{\phi}_j(s) = \Phi(z)$ and $\hat{\phi}_{j\pm 1}(s) = \Phi(z \mp 1)$; i.e., there is no phase shift between adjacent eigenmodes centered at each mode-rational surface. Equation (2) then reduces to a one dimensional differential-difference equation

$$[L_1 + \bar{Q} - \epsilon_n T_1 / \Omega] \Phi(z) = 0 \quad (3)$$

where $L_1 = b_\theta (\hat{s}^2 d^2 / dz^2 - 1)$

$$T_1 \Phi(z) = \Phi(z+1) + \Phi(z-1) + \hat{s} d/dz [\Phi(z-1) - \Phi(z+1)]$$

Equation (3) is the eigenmode equation describing collisionless

drift waves in toroidal plasmas. We also note that Equation (3) yields perturbations centered at the outside of the torus. The boundary condition imposed on equation (3) is that for large z , the outgoing wave decays asymptotically because of the onset of ion Landau damping.

To proceed from here, we approximate the ion Z function by

$$1 + \xi_i Z(\xi_i) = -1/2 \xi_i^2 + i\sqrt{\pi} \xi_i \exp(-\xi_i^2)$$

since $|\xi_i| \gg 1$. Equation (3) can then be written in the form:

$$[L_1 + Q_1 - \bar{W}(z)]\phi(z) = 0 \quad (4)$$

where $Q_1\phi(z) = [(1-\Omega)/(\Omega+1/\tau) + z^2/\Omega^2 n_s^2 - \epsilon_n T_1/\Omega]\phi(z)$,

and $\bar{W}(z) = [(1-\Omega)/(\Omega + 1/\tau)] \xi_e Z(\xi_e) - i\sqrt{\pi}\tau \xi_i \exp(-\xi_i^2)$.

Fourier transforming equation (4), we obtain

$$[d^2/d\eta^2 + Q(\Omega, \eta) - W] \hat{\phi}(\eta) = 0 \quad (5)$$

where $\hat{\phi}(\eta)$ is the Fourier transform of $\phi(z)$,

$$Q(\Omega, \eta) = \Omega^2 n_s^2 [b_\theta(1 + \hat{s}^2 \eta^2) - (1-\Omega)/(\Omega + 1/\tau)$$

$$+ 2(\epsilon_n/\Omega) (\cos \eta + \hat{s} \eta \sin \eta)],$$

$$W\hat{\phi}(\eta) = \int \Omega^2 n_s^2 \bar{W}(z) \phi(z) \exp(-inz) dz.$$

To analyze equation (5), we temporarily ignore the electron and ion dissipations and we have

$$[d^2/d\eta^2 + Q(\Omega_0, \eta)] \hat{\phi}_0(\eta) = 0 \quad (6)$$

The relevant boundary condition for equation (6) is then, $\hat{\phi}_0(\eta) \propto \exp(i \Omega_0 n_s b_\theta \hat{s} \eta^2 / 2)$ as $|\eta| \rightarrow \infty$, i.e., the wave energy is outward propagating. Equation (6) has been studied extensively⁵ for $\tau = \infty$, by using both the interactive WKB⁸ and numerical shooting codes. It has been shown that there exist two damped

eigenmode branches. One is slab-like and the other is a new branch induced by finite toroidicity. The slab-like eigenmodes, similar to the Pearlstein-Berk modes found in the slab limit,² have basically anti-well potential structures as shown in Fig. (1a) and therefore experience finite shear damping. This branch does not exist for $\hat{s} < \hat{s}_c$ and toroidicity further enhances the shear damping rates. The toroidicity induced (T-I) eigenmodes correspond to eigenstates quasi bounded by local potential wells. Depending on \hat{s} for fixed ϵ_n , the potential structure for weak T-I (large \hat{s}) eigenmodes is shown in Fig. (1b) and for strong T-I (small \hat{s}) eigenmodes is shown in Fig. (1c). It is clear that shear damping can occur through tunneling leakages and is, in general, negligibly small with $-\Omega_i \sim O(10^{-3})$. It is also interesting to note that both eigenmode branches can coexist for a certain parameter regime. Furthermore, we note that the slab-like eigenmodes have turning points $\pm\eta_t$ close to $\eta = 0$, i.e., $|\eta_t| \ll 1$, and therefore can be understood by using Taylor's strong-coupling approximation. On the other hand, the T-I eigenmodes cannot be described by the strong-coupling approximation. We now proceed to show that electron dissipation can destabilize the T-I eigenmodes.

Since tokamaks typically have large shear, $\hat{s} > 1/2$, we will concentrate our analytic theory on weak T-I eigenmodes. From Fig. (1b), we can readily see that the eigenmodes will be localized around $\eta = \eta_0 \neq 0$ where $Q'(\eta_0) = 0$, i.e.,

$$b\hat{s}^2\eta_0 + (\epsilon_n/\Omega)[(\hat{s}-1)\sin\eta_0 + \hat{s}\eta_0 \cos\eta_0] = 0. \quad (7)$$

Letting $\theta = \eta - \eta_0$, we can expand Q about η_0 to $O(\theta^2)$ and equation (5) becomes

$$[\frac{d^2}{d\theta^2} + Q(\eta_0) + Q''(\eta_0)\theta^2/2 - w] \hat{\phi}(\eta) = 0 \quad (8)$$

where $\text{Re}Q''(\eta_0) < 0$. Inverse Fourier transforming equation (8) and setting $\phi(t) = \frac{1}{2\pi} \int d\theta \hat{\phi}(\eta) \exp(i\theta t) = \phi(t) \exp(-i\eta_0 t)$, we obtain

$$[-(1/2)Q''(\eta_0)d^2/dt^2 + Q(\eta_0) - t^2 - \Omega^2 \eta_s^2 \bar{W}(t)]\phi(t) = 0 \quad (9)$$

Equation (9) can be rewritten as

$$[d^2/dy^2 + \lambda - y^2 - \Lambda] \phi(y) = 0 \quad (10)$$

where $y = t/(-Q''(\eta_0)/2)^{1/2}$, $\lambda = Q(\eta_0)/\sqrt{-Q''(\eta_0)/2}$, $\Lambda = \Omega^2 \eta_s^2 \bar{W}(t)/\sqrt{-Q''(\eta_0)/2}$. Taking $\Lambda(t)$ to be small compared with λ and y^2 , which will be justified by comparing with numerical results, we can carry out a perturbative treatment of equation (10) and obtain the zeroth order solution

$$\phi_0(y) = \exp(-y^2/2) \quad (11)$$

for the $n = 0$ eigenstate. The corresponding dispersion relation is given by

$$Q(\eta_0)/\sqrt{-Q''(\eta_0)/2} = 1 \quad (12)$$

To further analyze equation (12) we need to obtain η_0 from equation (7). Since weak T-I eigenmodes generally exist for $|\varepsilon_n/\Omega| > |b_\theta \hat{s}|$, and $|\eta_0| > 1$, we find $\eta_0 \approx \pi/2$ for $\hat{s} \sim 1$. Thus, $Q(\eta_0) \approx \Omega^2 \eta_s^2 [1 + b_\theta (1 + \hat{s}^2 \pi^2/4) - \frac{(1+1/\tau)}{(\Omega+1/\tau)} + \hat{s} \varepsilon_n \pi/\Omega]$ and

$$\sqrt{-Q''(\eta_0)/2} \approx \Omega \eta_s [\varepsilon_n \hat{s} \pi/2\Omega - b_\theta \hat{s}^2]^{1/2} \quad (14)$$

The solution of equation (12) can be obtained for $(\varepsilon_n \hat{s} \pi/2\Omega - b_\theta \hat{s}^2) \ll 1$ and $\tau \ll 1$, and is approximately given by

$$\eta_0 \approx (1 - \hat{s} \varepsilon_n \pi) / [1 + b_\theta (1 + \hat{s}^2 \pi^2/4)] \quad (15)$$

With the addition of the Λ term, we obtain the dispersion relation

$$Q(\eta_0)/\sqrt{-Q''(\eta_0)/2} \approx 1 + i(\Gamma - \delta), \quad (16)$$

where δ is included to represent shear damping effects through tunneling leakages and can be estimated by examining the $W = 0$ limit of equation (5) and

$$\Gamma(\Omega) = \int \Lambda \phi_0^2 dy / \int \phi_0^2 dy.$$

To obtain an analytical expression for Γ , we approximate the electron Z function by retaining only the resonant term, and have

$$\Gamma = 4\alpha^3 \{ [(1-\Omega)/(\Omega+1/\tau)] (d/\tau) K_0(2d\alpha) - K_0(2\alpha) \}, \quad (17)$$

where $\alpha = \Omega n_s \sqrt{\tau/2} / (-Q''(\eta_0)/2)^{1/4}$, and K_0 is the modified Bessel function of the second kind. For typical tokamak parameters, we find $\alpha \gg 1$ and $d\alpha \ll 1$, so that

$$K_0(2d\alpha) \approx -\ln(d\alpha) - C, \quad (18)$$

where $C (= 0.5772\dots)$ is Euler's constant, and

$$K_0(2\alpha) \approx 1.25 (2\alpha)^{-1/2} \exp(-2\alpha). \quad (19)$$

We note that $|\Gamma| \ll 1$. Thus, with $\Omega = \Omega_0 + i\Omega_i$ and $|\Omega_i/\Omega_0| \ll 1$, we have, from equation (16),

$$\Omega_i \approx \beta \{ 4\alpha^3 [(d/\tau) (1-\Omega_0) / (\Omega_0 + 1/\tau) (-\ln(d\alpha) - C) - 1.25 (2\alpha)^{-1/2} \exp(-2\alpha)] - \delta \} \quad (20)$$

where

$$\beta = (\epsilon_n \hat{s} \pi / 2\Omega_0 - b_\theta \hat{s}^2)^{1/2} / [n_s (1 + b_\theta (1 + \hat{s}^2 \pi^2 / 4))].$$

Examining equation (20), we find that the electron Landau damping term has a destabilizing effect and is proportional to $\sqrt{m_e/m_i}$, while the ion Landau damping term is stabilizing and is independent of the mass ratio.

We have also solved the differential-difference equation (Eq. 3) numerically by using the cubic B-spline finite element method⁹ in order to verify the perturbative treatment and provide more understanding. Numerical results are exhibited in Figs. (2a) and (2b) for $b_\theta = \varepsilon_n = 0.1$, $\beta = 1$, $\tau = 10$, $m_i/m_e = 1837$. For this set of parameters we note from the analysis⁵ of equation (6) that weak T-I eigenmodes exist for $\hat{s} \gtrsim 0.5$. In Fig. (2a) we plot the growth rate versus shear \hat{s} and the real frequency is plotted in Fig. (2b). Five curves are compared: (a) the numerical solutions of equation (3) for T-I eigenmodes; (b) numerical solutions of equation (3) for slab-like eigenmodes; (c) numerical solutions of equation (3) in the slab limit, i.e., $T_1 = 0$; (d) perturbative solutions for weak T-I eigenmodes; equations (12) and (20) by neglecting tunneling effects, i.e., $\delta = 0$; (e) numerical solution of equation (3) in the strong-coupling limit, i.e., $T_1 \Phi(z) \approx 2\Phi + (1-2\hat{s})(d^2/dz^2)\Phi$. The results clearly demonstrate that, while in the slab limit the eigenmodes are always stable, T-I eigenmodes become unstable for $\hat{s} \lesssim 1.2$ and slab-like eigenmodes experience enhanced damping due to finite toroidicity compared with the eigenmodes in the slab limit. We also note that for T-I eigenmodes the agreement between perturbation theory and numerical results is reasonably good for Ω_i . They both predict instability for $\hat{s} \lesssim 1.2$ for the set of parameters presented here. In order to further justify the perturbative analysis for T-I eigenmodes, we have also numerically solved equation (3) by artificially inserting a factor λ_e in the electron nonadiabatic term $\xi_e Z(\xi_e)$ and varied λ_e from zero to one.

We found that, as an example, for $s = 0.75$, ω_i evolved from negative (damping) at $\lambda_e = 0$ to positive (instability) at $\lambda_e = 1$, and is linear in λ_e . We also emphasize that the strong-coupling approximation predicts fairly well the damping rates for the slab-like branch for $s > 0.5$; however, it fails to account for the instability of the T-I eigenmodes. Finally, we note that even though only the $\tau = 10$ case is presented, the basic results are not changed for $\tau \sim 0(1)$.

Acknowledgments

The authors would like to thank Dr. G. Rewolut for useful discussions.

REFERENCES

* Work supported by the United States Department of Energy, Contract EY-76-C-02-3073.

¹D. W. Ross and S. M. Mahajan, *Phys. Rev. Lett.* 40, 324 (1978); K. T. Tsang, P. J. Catto, J. C. Whitson and J. Smith, *Phys. Rev. Lett.* 40, 327 (1978); Liu Chen, P. N. Guzdar, R. B. White, P. K. Kaw and C. Oberman, *Phys. Rev. Lett.* 41, 649 (1978).

²L. D. Pearlstein and H. L. Berk, *Phys. Rev. Lett.* 23, 220 (1969).

³J. B. Taylor, in *Proc. of 6th Int. Conf. on Plasma Physics and Controlled Nuclear Fusion Research*, Vol. 2 (IAEA, Vienna, 1977), p. 323.

⁴Liu Chen, P. N. Guzdar, J. Hsu, P. K. Kaw, C. Oberman, and R. B. White, *Nucl. Fusion* 19, 373 (1979); W. Horton, R. D. Estes, H. Kwak and D. I. Choi, *Phys. Fluids* 21, 1366 (1978).

⁵Liu Chen and C. Z. Cheng. *Princeton Plasma Physics Laboratory Report PPPL-1562* (1979).

⁶J. W. Connor, R. J. Hastie and J. B. Taylor, *Culham Laboratory Report CLM-P537* (1978); A. H. Glasser, in *Proc. Finite Beta Theory Workshop*, Varenna, 1977, ed. B. Coppi and W. Sadowski.

⁷W. M. Tang, *Nucl. Fusion* 18, 1089 (1978).

⁸R. B. White, *J. Compt. Phys.* 31, 3 (1979).

REFERENCES CONT'D.

⁹W. H. Miner, The Univ. of Texas, Fusion Research Center Report FRCR #138 (1977).

FIGURE CAPTIONS

Fig. 1. Typical potential structures $Q(\eta)$ for (a) the slab-like, (b) weak and (c) strong toroidicity induced eigenmodes.

Fig. 2. Plot of eigenmode frequencies ω versus δ for $b_0 = \epsilon_n = 0.1$, $q=1$, $\tau=10$, $m_i/m_e = 1837$. Curves (a), (b), (c) correspond, respectively, to T-I eigenmodes, slab-like eigenmodes and uniform plane slab eigenmodes from numerical solution of equation (3). Curve (d) corresponds to perturbative results for T-I eigenmodes and curve (e) to numerical solution of equation (3) in the strong-coupling approximation.

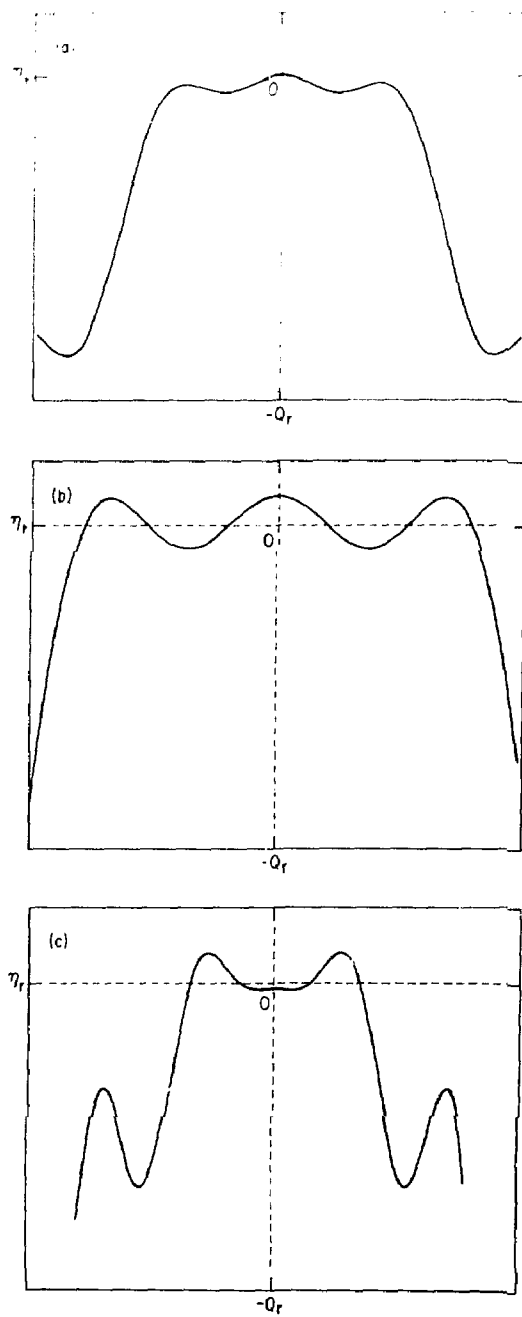


Fig. 1. 792375

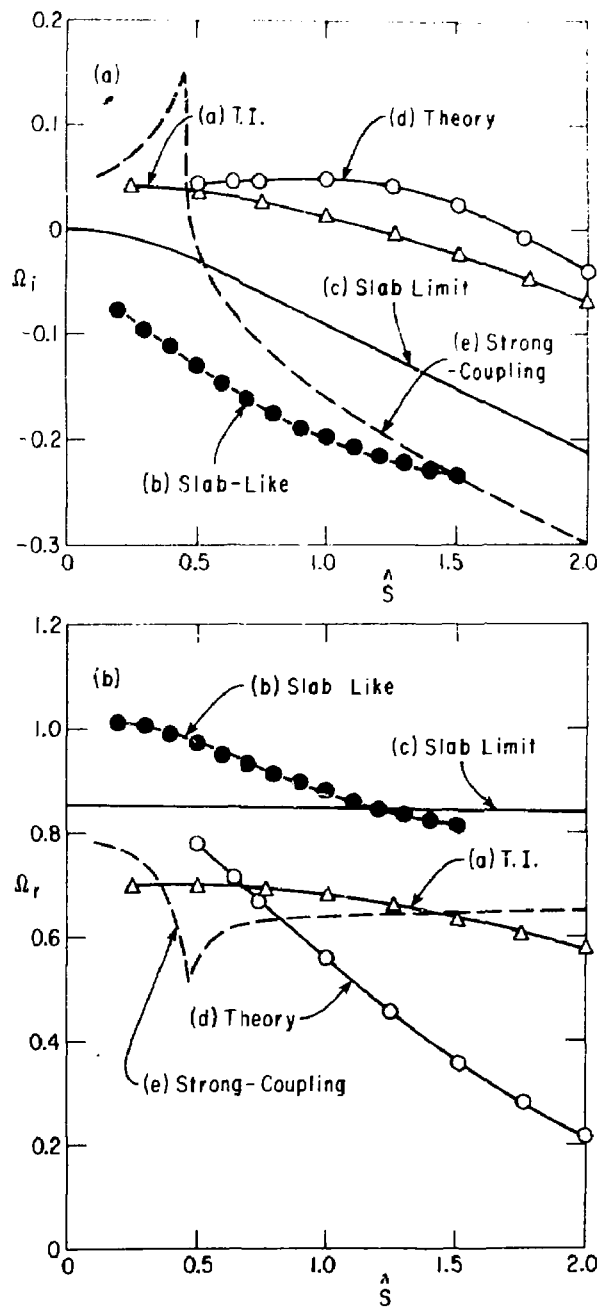


Fig. 2. 792374